

RSC Advances



This is an *Accepted Manuscript*, which has been through the Royal Society of Chemistry peer review process and has been accepted for publication.

Accepted Manuscripts are published online shortly after acceptance, before technical editing, formatting and proof reading. Using this free service, authors can make their results available to the community, in citable form, before we publish the edited article. This *Accepted Manuscript* will be replaced by the edited, formatted and paginated article as soon as this is available.

You can find more information about *Accepted Manuscripts* in the [Information for Authors](#).

Please note that technical editing may introduce minor changes to the text and/or graphics, which may alter content. The journal's standard [Terms & Conditions](#) and the [Ethical guidelines](#) still apply. In no event shall the Royal Society of Chemistry be held responsible for any errors or omissions in this *Accepted Manuscript* or any consequences arising from the use of any information it contains.

Mesenchymal stem cell response to UV-photofunctionalized TiO₂ coated CoCrMo

Niall Logan¹, Alison J Cross², Alison Traynor³, Laurent Bozec¹, Ivan P Parkin², Peter Brett^{1*}

¹ Biomaterials and Tissue Engineering,
University College London, Eastman Dental Institute,
256 Gray's Inn Road,
London, WC1X 8LD

² Department of Chemistry
University College London
20 Gordon Street
London, WC1H 0AJ

³ Corin Ltd,
Cirencester,
Gloucestershire,
GL7 1YJ

*Corresponding Author

Email p.brett@ucl.ac.uk; Tel:- 0044(0)203 4561104

Abstract

Ultraviolet (UV) photofunctionalization has been shown to be highly effective at improving the osteoconductivity of titanium and TiO₂ coated materials. We aimed to assess whether the bioactivity of TiO₂ coated cobalt chromium molybdenum (CoCrMo) could be enhanced by UV photofunctionalization of the surface TiO₂ layer. Using atmospheric pressure chemical vapour deposition (APCVD) a thin layer of anatase TiO₂ was deposited onto smooth CoCrMo discs (Referred to as CCMT). Human mesenchymal stem cells (MSCs) were cultured onto CCMT substrates which had been treated with UV light for 24 hours and identical substrates which had not undergone UV treatment. UV treated CCMT promoted a superior cell response in the form of enhancing markers of cell adhesion. This included stimulating the development of larger cells with increased levels of the adhesion protein vinculin and cytoskeletal protein f-actin ($p < 0.05$). In addition, MSCs were shown to have superior retention to UV treated CCMT after 3 and 24 hours ($p < 0.05$). Other cellular processes including proliferation, attachment, migration and differentiation were not affected by UV photofunctionalization. Despite this, the enhancement in cellular adhesion alone should result in an improvement in MSC retention to implant surfaces following surgery, and as a consequence, increase MSC resistance to dislodgement from external forces such as blood flow and micro motion.

Introduction

The field of biomaterials continues to receive widespread attention as the need for medical devices with increased longevity and bioactivity intensifies. This is prominent in the field of orthopaedics, which is predicted to see a strong rise in the amount of total hip and knee replacement procedures performed by 2030¹. Furthermore, revision surgery is set to follow this trend, placing increased pressure on the industry, both clinically and economically^{2,3}. To cope with this anticipated situation, improving current generation biomaterials is a high priority and can be achieved by methods such as surface modification. We have previously shown that coating cobalt-chromium-molybdenum (CoCrMo) in a layer of anatase TiO₂ by APCVD, can improve the osteogenic differentiation and adhesion of human mesenchymal stem cells (MSCs) *in vitro*⁴. This improvement to cellular behaviour is thought to be due to the TiO₂ layer masking the underlying CoCrMo alloy, preventing the MSCs from interacting with the CoCrMo. In place of the CoCrMo, the MSCs are thought to be mediated by the TiO₂ coating; the same naturally occurring oxide layer as found on titanium and its alloys, which are widely accepted as the material of choice for orthopaedic and dental applications, although they do not have the mechanical strength of CoCrMo⁵.

TiO₂ is highly photoreactive and upon irradiation by ultraviolet (UV) light it transitions from partially hydrophobic to super-hydrophilic (water contact angle of $< 5^\circ$)⁶. The hydrophilicity, or surface free energy of a substrate, is thought to play a pivotal role in the initial events that take place after implantation. Materials that are identical in topography, yet only differ in surface wettability, have shown that those which are super-hydrophilic have superior bioactivity, both *in vitro*⁷⁻⁹ and *in vivo*¹⁰⁻¹⁷. The conversion of bulk titanium from hydrophobic to super-hydrophilic by way of UV irradiation has adopted the term 'UV photofunctionalization'. UV photofunctionalized bulk titanium has been shown to increase cellular proliferation, migration, adhesion and differentiation *in vitro*¹⁸, as well as promote superior bone implant contact¹⁹ and enhance bone formation in a gap healing model *in vivo*²⁰. In addition, the recently discovered time dependent degradation of biomaterial osteoconductivity²¹, can be reversed to its initial level of bioactivity, and even further improved upon by UV photofunctionalization^{22,23}. This phenomena is not restricted to pure titanium substrates and has been observed on other materials coated with TiO₂, which when photofunctionalized, enhanced cell attachment, adhesion and bone apposition^{24,25}.

Despite these promising conclusions, the underlying mechanisms regarding UV-photofunctionalization are not well understood. Recent publications have suggested that UV photofunctionalization may change the electrostatic potential of the surface, converting the charge of non-UV treated titanium surfaces from electronegative to electropositive^{26,27}. Other mechanisms have been proposed, including that UV irradiation causes the removal and/or decomposition of contaminating hydrocarbons from the material surface^{28,29}, or that surface oxygen vacancies at bridging sites are created, resulting in the conversion of Ti⁴⁺ sites to Ti³⁺ sites, which are favourable for dissociative water adsorption⁶.

Despite the mechanisms behind UV-photofunctionalisation remaining still not fully understood, the present study aimed to test the hypothesis that UV-photofunctionalized CCMT would enhance the cellular performance of human MSCs *in vitro*, compared to identical substrates which had not undergone UV irradiation. In particular, this study examined markers of cell attachment, retention, migration, proliferation and differentiation, as well as the expression of adhesion and cytoskeletal protein structure using fluorescent microscopy.

Materials and Methods

Sample preparation

CoCrMo discs (Cr 26-30, Mo 5-7) of \varnothing 15 mm and 1 mm thickness, were supplied with a machined finish by Corin Ltd (Cirencester, UK). To remove this topography, individual discs were ground and polished to a smooth finish as previously described⁴. To prepare substrates for cell culture experiments, discs were put in nitric acid (0.1 N, BDH, 19088 5E) for 10 minutes, washed thoroughly in ddH_2O and allowed to air dry. Non-UV CCMT substrates were then irradiated with UVC light for 20 minutes on each side (BONMAY, BR-506) and kept in a sterile environment for 48 hours to allow recovery to a hydrophobic state. UV-treated CCMT samples were irradiated with UVC light for 24 hours and used immediately for cell culture experiments.

Chemical vapour deposition

Titanium tetrachloride (TiCl_4) and ethyl acetate were used to create the thin film TiO_2 coatings on CoCrMo via APCVD as previously described⁴. The process followed a procedure developed by us previously to coat both glass and steel substrates^{30,31}. X-ray diffraction, x-ray photoelectron spectroscopy and Raman spectroscopy were performed to confirm the presence of anatase TiO_2 (Not shown here).

Cell culture

Human MSCs from three donors were obtained from the Institute for Regenerative Medicine, Texas A&M Health Science Center College of Medicine, USA. Pre-characterisation of the MSCs had been performed which included the expression of stem cell surface markers, and osteogenic, adipogenic and chondrogenic differentiation. Cells were seeded on tissue culture plastic at a density of 740 cells cm^{-2} and expanded in growth medium (GM) that comprised of Minimum Essential Medium α (Gibco, 22571-020) containing 10% fetal bovine serum (Invitrogen, 10270106) and 1% penicillin/streptomycin (Sigma-Aldrich, P0781). MSCs were incubated at standard culture conditions of 37°C/5% CO_2 in a humidified atmosphere with media changed every 3 - 4 days. When cells reached 80% confluence they were harvested by treatment of Trypsin (0.05%)/EDTA(0.002%) (Life technologies, R-001-100). Only cells of low passage (<5) were used to ensure integrity of the results. When osteogenic media (OM) was implemented, it consisted of Dulbecco's Modified Eagle's Medium (DMEM) low glucose pyruvate (Gibco, 31885-023), containing 10% fetal bovine serum, 1% penicillin/streptomycin and further supplemented with β -glycerol phosphate (Sigma-Aldrich, G9891), L-ascorbic acid (Sigma-Aldrich, A8960) and dexamethasone (Sigma-Aldrich, D9402).

Contact Angle

To measure the wettability of the non-UV and UV-treated CCMT samples ($n = 5$), contact angle measurements were performed using an optical contact angle meter (KSV Instruments LTD, CAM 200) with 2 μl drops of ddH_2O . Measurements were taken over a time course during UV exposure up to 24 hours and post exposure until 48 hours.

Fourier Transform Infrared Spectroscopy (FTIR)

FTIR analysis (Perkin Elmer, System 2000) was performed on CCMT substrates ($n = 5$) both before and after 24 hours exposure to UVC light to ascertain if there was any reduction in hydrocarbon content on the substrate surface. Spectra were taken in the range 3100 – 2700 cm^{-1} using an average of 16 scans per sample.

Cell proliferation

MSCs from three donors were seeded at 2×10^3 cells per well ($n = 3$) in both GM and OM and incubated at 37°C/5% CO_2 in a humidified atmosphere with media changes every 3-4 days. The amount of cells at different time points was assessed using AlamarBlue (AbD Serotec); 100 μl of oxidised dye was added to each well containing 1 ml of media and cells were incubated for 4 hours at standard culture conditions before having two 100 μl aliquots of supernatant removed from each well for analysis. The fluorescent intensity of the dye was measured (Excitation $\lambda = 530$ nm, emission $\lambda = 590$ nm, BioTek FLX800) and cell numbers calculated via interpolation through use of a seven point standard curve, ranging to a maximum of 10×10^4 cells per well.

Cell attachment

To analyse the capability of both UV treated and non-UV CCMT to promote cell attachment, MSCs from three donors were seeded at a density of 3×10^4 ($n = 3$) in GM and incubated at standard culture conditions for 24 hours. Following this, the media was replaced and cells counted using AlamarBlue as previously described.

Cell retention

To gain an understanding of how well adhered the attached cells were to the substrates, a cell retention study was performed. MSCs from three donors were seeded at 3.5×10^4 cells per well ($n = 3$) in GM and incubated at 37°C/5% CO_2 in a humidified atmosphere. After 3 and 24 hours incubation, MSCs were washed thoroughly 3 times with PBS on an orbital shaker (60

seconds at 60rpm), and then using the same method as previously described, the remaining cells were quantified via AlamarBlue assay.

Cell Migration

A cell migration assay (Cultrex, 3465-024-K) was used to ascertain if the practice of UV photofunctionalization had the potential to enhance the migratory capability of the cell population. MSCs from three donors were serum starved for 24 hours prior to performing the assay and following this, were seeded at 7.5×10^4 cells per well ($n = 3$) into the top chamber of the insert, which contained a polymer membrane with $8\mu\text{m}$ pores to allow cell invasion. $500\ \mu\text{l}$ of GM was placed into the bottom chamber of the inserts and the cells were incubated at standard culture conditions for 4.5 hours. Substrates were then washed three times with wash buffer and incubated at 37°C for 60 minutes with cell dissociation solution containing Calcein AM. Two $100\ \mu\text{l}$ aliquots were then taken from each well and the fluorescent intensity measured (Excitation $\lambda = 485\ \text{nm}$, emission $\lambda = 520\ \text{nm}$). Cell numbers were calculated via interpolation through use of a standard curve.

Cell morphology

F-actin and the adhesion protein vinculin, were labelled with fluorescent markers and viewed under a fluorescence microscope to analyse the morphology of the cells on UV treated and non-UV CCMT. MSCs were seeded at 5×10^3 cells per well in OM ($n = 3$). After 24 hours in culture, cells were fixed using 4% paraformaldehyde for 15 minutes, then treated with 0.15% Triton X-100 (BDH, 30632 4N) in Dulbecco's phosphate buffer saline (PBS) for 4 minutes to permeabilise the cellular membrane. The MSCs were then blocked using 10% goat serum in PBS for 30 minutes to prevent any unspecific binding. Primary antibody incubation was performed overnight at 4°C using the anti-vinculin antibody (Abcam, ab18058, 1:200). Alexa fluor 568 goat anti-mouse (Molecular probes, A11031, 2.5:100) was then used as a secondary antibody, with all primary and secondary antibodies diluted in 1.5% skim milk in PBS. Lastly, MSCs were counterstained with alexa fluor 488 phalloidin in PBS (Molecular probes, A12379, 2.5:100). Images were taken using a fluorescent microscope fitted with the appropriate filters (Leica DMIRB) and then quantifiable analysis was performed via a pixel based method using ImageJ software.

Mineralisation

Markers linked to both early and late stages of osteogenesis were studied. MSCs from three donors were seeded at a density of 2×10^4 cells per well ($n = 3$) in OM and examined at 6 days for alkaline phosphatase (ALP) activity and 21 days for both calcium and hydroxyapatite.

The ALP activity was normalised to a per cell level by quantifying the amounts of cells prior to performing the assay as previously described. The ALP activity was assessed using a colorimetric assay (Abcam, ab83369) as per the manufacturer's instructions. MSCs were washed twice with PBS before being dissociated from the substrates by treatment with trypsin. MSCs were then centrifuged at 13,000 rpm for 6 minutes to form a pellet, before being resuspended in $200\ \mu\text{l}$ of assay buffer by use of a vortex and left for 15 minutes to allow the buffer to effectively lyse the cells. $80\ \mu\text{l}$ of each sample was then transferred to a clear 96 well plate and combined with $50\ \mu\text{l}$ of 5 mM *p*-nitrophenyl phosphate (*p*NPP). After 60 minutes incubation at room temperature in the dark, $20\ \mu\text{l}$ of stop solution was added to all samples and the optical density was measured at 405 nm (Tecan, M200). Concentrations were calculated with the use of known concentration standards.

Calcium ion content was studied using the QuantiChrom calcium assay (Bio Assay systems, DICA-500). Prior to performing the assay the amounts of cells were assessed as previously described. The cell monolayer was washed twice using PBS and homogenised by incubation with $500\ \mu\text{l}$ 1M hydrochloric acid (HCl) for 60 minutes at room temperature on a rocking plate. Aliquots were then taken from each sample and transferred to a clear 96 well plate and combined with assay reagent. Calcium levels were measured ($\lambda = 620\ \text{nm}$, Tecan M200) and concentrations calculated with use of known concentration standards.

The total amounts of hydroxyapatite formed on substrates as measured using the OsteoImage mineralisation assay (Lonza, PA-1503). MSCs were washed twice in PBS and fixed using 4% paraformaldehyde for 15 minutes. Following this the cells were then washed twice with diluted wash buffer and incubated in the dark for 30 minutes at room temperature with staining reagent. The MSCs were then washed three more times with diluted wash buffer and the amounts of hydroxyapatite quantified using a fluorescent plate reader (Excitation $\lambda = 492\ \text{nm}$, emission $\lambda = 520\ \text{nm}$, BioTek FLX800). Visual inspection of hydroxyapatite nodules was then performed using a fluorescence microscope (Leica DMIRB).

Statistical analysis

For this study human MSCs from three donors ($N = 3$) were used in triplicate ($n = 3$). Contact angle studies were performed at $n = 5$, and cytometric analysis was performed at $n = 13$. Statistical analysis was carried out using the student t test in GraphPad Prism software (v5.04), with $p < 0.05$ deemed to be statistically significant.

Results

Contact angle

The photo-reactivity of the CCMT discs was analysed by examining the water contact angle on the substrate following exposure to UV light over time (Figure 1). The water contact angle of a substrate is a measure of the wettability of the sample, which can be referred to as the substrate surface energy. CCMT discs had a time zero (T0) contact angle of $61.62^\circ \pm 8.70^\circ$ which rapidly decreased to $9.44^\circ \pm 6.21^\circ$ after 60 minutes of UV light exposure. By 4 hours, the water contact angle had reduced further to $5.10^\circ \pm 0.98^\circ$ and then ultimately became super-hydrophilic ($< 5^\circ$) after 24 hours exposure to UV light.

The recovery of the water contact angle on CCMT, from super-hydrophilic back to hydrophobic, was studied using the same process (Figure 2). Removing the substrates from the UV chamber, after 30 minutes the contact angle had increased from 0° to $12.17^\circ \pm 4.85^\circ$. By 6 hours this had increased further to $40.45^\circ \pm 9.82^\circ$. After 48 hours the water contact angle returned to its original T0 surface energy value of $61.53^\circ \pm 6.71^\circ$.

FTIR

There was no apparent difference in the peak intensities of methylene hydrocarbon groups on CCMT substrates following UV irradiation with UVC light for 24 hours (Figure 3).

Cell proliferation

Proliferation in OM was examined over a three week time course (Figure 4). A slow rate of proliferation was observed on both UV-treated and non-UV substrates from day 1 to day 7. Following this, the minor decrease that was observed on both surfaces is possibly due to contact inhibition or apoptosis triggered from the differentiation process. A similar amount of cells was found at day 21 compared to day 1. No significant differences were observed between the two substrates.

The proliferation of MSCs in GM did not seem to be affected by the UV photofunctionalisation of the CCMT surface (Figure 5). Both non-UV and UV treated CCMT substrates promoted a similar level of proliferation up until 21 days in culture, with no significant differences between the two substrates being observed.

Cell attachment

The number of attached cells after 24 hours in culture did not differ between the substrates, as shown in figure 6. UV treated CCMT was shown to have a similar amount of attached cells (19460 ± 4802) as found on non-UV CCMT (19518 ± 6051).

Cell retention

Cell retention to the substrates was analysed by quantifying the remaining cell populations after incubation time periods of 3 and 24 hours, where the MSCs were then washed three times with PBS before being quantified. It was found that significantly more cells remained on the UV-treated CCMT (8183 ± 1382) substrate compared to non-UV CCMT (7017 ± 1194) after 3 hours, as shown in figure 7. This effect was again evident at 24 hours, with significantly more cells remaining on UV treated CCMT (18333 ± 5745) over the non-UV substrate (15250 ± 2557).

Cell Migration

The use of UV photofunctionalization as a chemotactic factor to enhance cell migration was studied after 4.5 hours incubation (Figure 8). The migration and colonisation of MSC populations was successful on both non UV (13681 ± 4370) and UV treated substrates (12847 ± 4419) although no significant difference between substrate groups was observed.

Cell Morphology

Fluorescent microscopy analysis of MSCs on both substrates after 24 hours in OM showed discernible differences in cell morphology between the two substrates (Figure 9). The MSC population were larger and more spread on UV-treated CCMT substrates. The non-UV substrate did still promote cytoskeletal re-organisation and the promotion of protrusions in the form of lamellipodia, although the MSCs were clearly smaller compared to those found on UV-treated CCMT. Actin fibres in MSCs on the UV-treated surface appeared to be more robust and better developed than those observed on non UV substrates (Figure 9 – A-B). Due to increase in cell size on the UV treated CCMT substrate, vinculin was more widely expressed within the cell, with a greater number of focal adhesions per cell (Figure 9 – D).

Cytomorphology was carried out on cells on both non-UV and UV-treated CCMT substrates (Figure 10). MSCs on the UV-treated CCMT surface were larger and had a significantly greater cell perimeter to those found on the non-UV surface. The ferets diameter of individual cells was also analysed, although no significant difference was observed between the two groups. The expression of actin and the focal adhesion protein vinculin were also analysed using ImageJ. MSCs found on the UV-treated CCMT substrate had significantly greater actin expression over those found on non-UV CCMT. This trend was also observed with the adhesion protein vinculin, with MSCs on the UV-treated CCMT again displaying increased levels of expression over MSCs found on non-UV CCMT substrates.

Mineralisation

The level of osteogenic differentiation occurring in MSCs can be directly related to mineralisation and one method of monitoring this process is by analysing certain markers of this phenomenon. ALP activity plays a role in early stage osteogenesis³², whilst calcium ion content and hydroxyapatite are commonly used as late markers. There was no significant difference in either early or late stage markers of osteogenesis between UV-treated or non-UV CCMT substrates (Figure 11). In addition, visual inspection of hydroxyapatite formation on the substrates via fluorescent microscopy, showed no apparent difference in hydroxyapatite formation and structure.

Discussion

Coating the bio-inert orthopaedic material, CoCrMo, in a layer of TiO₂ has been shown to improve the bioactivity of the material by enhancing the osteogenic differentiation and adhesion of human MSCs⁴, and improving the gene expression and actin formation of human endothelial cells³³. As a result, TiO₂ coating techniques may have the capability to improve CoCrMo implant performance by increasing the colonisation and differentiation potential of cells capable in facilitating in bone healing and formation. The present study investigated if it were possible to improve upon this response, by functionalizing the surface TiO₂ layer of CCMT by way of UV irradiation. The phenomenon, which has been adopted the term 'UV photofunctionalization', converts the material from hydrophobic to super-hydrophilic via irradiating the surface of the substrate with UV light and has been reported to significantly improve cellular response compared to non-UV treated substrates^{18-20, 24, 25, 34, 35}, as well as been shown capable of reversing the effects of the recently discovered time dependant degradation of biomaterial osteoconductivity²¹⁻²³. In addition, UV irradiation of TiO₂ has bactericidal and detoxifying properties that may prove advantageous for orthopaedic application where infection is a common failure mechanism³⁶.

The effect of UV photofunctionalization on CCMT was not consistent among the different experiments completed in this study, stimulating an improvement in some tests, but having no significant impact in others. Osteogenic differentiation, proliferation, migration and attachment were unaffected by UV photofunctionalization of CCMT (Figures 4-7 & 11). In contrast, in a study by *Aita et al*, significant improvement to these processes were reported using human MSCs on UV photofunctionalized acid etched titanium¹⁸. It was also shown that MSCs found on UV functionalized titanium were larger, which as a consequence, had increased expression of the focal adhesion protein vinculin and the cytoskeletal protein f-actin. Interestingly, this cellular response was present on UV photofunctionalized CCMT (Figure 9) and has been observed in many separate studies^{18, 19, 24, 26, 34, 35, 37}. This implies that UV photofunctionalization of CCMT is having an impact at the cellular level, although it is promoting a different, considerably less dynamic response compared to that found on UV photofunctionalized titanium and Ti6Al4V. This is an interesting discovery, as the TiO₂ layer used in the present study to coat the CoCrMo discs, is the same naturally occurring oxide layer as found on titanium and its alloys³⁸, implying that UV photofunctionalization is not mediated solely by the surface oxide layer, but is also influenced by the bulk of the material. It should be pointed out that the thickness of the TiO₂ coating on CCMT is greater than that found on native bulk titanium which may be influential towards the variation observed.

UV photofunctionalization of TiO₂ layers have also been studied by *Miyauchi et al*²⁴. Using TiO₂ layers deposited onto glass plates via a sputter coating technique, *Miyauchi et al* was able to show significant improvement in cell size, density, proliferation, attachment and adhesion in bone marrow cells from Sprague-Dawley rats. This strong increase in cellular response to UV photofunctionalized TiO₂ layers was not detected to the same extent in the present study, as proliferation and attachment were not affected, although an improvement in the form of increased cell retention and size was observed (Figures 7 & 10). This variation between studies is likely to be directly related to differences in cell type, deposition technique and the use of glass as the bulk material in place of CoCrMo.

The increased retention of MSCs at both 3 and 24 hours on UV photofunctionalized CCMT (Figure 7) can be used as an indirect measure of how well adhered each MSC is to the substrate surface. This data can therefore be correlated to the improvement in single cell adhesion forces reported by *Miyauchi et al*²⁴, supporting the observation of enhanced cell adhesion to UV photofunctionalized TiO₂ layers, an effect also observed on mirror polished titanium³⁴. Accelerated and superior actin fibre development (Figure 9-B), and increased levels of vinculin (Figure 9-D), are likely to be the cause of this enhancement in cellular adhesion. More robust, developed f-actin fibres have been shown to increase cellular stiffness³⁴, whilst vinculin forms focal adhesion complexes which connect the cytoskeletal structure of the cell, to adhesion membranous molecules³⁹. The combination of these two proteins being more extensively expressed is likely to promote stiffer, better adhered cells. This is highly advantageous for the field of orthopaedics, where cells that colonise onto the surface of the implant are exposed to several external forces, such as blood flow and micro motion.

Miyauchi et al also briefly studied UV photofunctionalized TiO₂ layers on other biomaterials, including CoCrMo and polytetrafluoroethylene (PTFE)²⁴. Increased cell attachment and ALP activity was reported on both materials which had been UV photofunctionalized, although it is not clear whether the ALP activity was normalised to a per cell level. Consequently, when taken into consideration the increased cell attachment and proliferation on UV photofunctionalized TiO₂ coated glass from the same study; it may be that this heightened ALP activity is a direct consequence of a larger cell population being present on the UV photofunctionalized substrate, rather than actual improvement in cellular ALP activity.

In the present study, markers of osteogenic differentiation, including calcium ion content, hydroxyapatite and ALP activity were shown to be unaffected by UV photofunctionalization of CCMT (Figure 11). Despite this, *Aita et al* have been able to demonstrate significant improvements in the differentiation of human MSCs on UV photofunctionalized titanium¹⁸. *Aita et al* established that the process of UV photofunctionalization does have the capability to improve the differentiation of stem cells on certain materials, and it may be that the TiO₂ layers created by *Miyauchi et al*²⁴, using a sputter coating technique, formed a more bioactive oxide layer capable of improving cellular differentiation. Contrarily, this conflict in results may merely be the consequence of the different cell type used or the ALP activity not normalized to a per cell level. Despite this, in the future it would be interesting to look at human MSC response to UV photofunctionalized TiO₂ coated CoCrMo, using a variety of different deposition techniques, including APCVD and sputter coating.

The mechanisms of UV photofunctionalization are still not entirely understood, although several possibilities have been proposed and investigated. *Carp et al* stated that upon UV irradiation, Ti⁴⁺ sites are converted to Ti³⁺ sites and in doing so, oxygen vacancies are formed at bridging sites which are more favourable for dissociative water adsorption^{6,40}. It has also been demonstrated that following UV photofunctionalization of titanium, the charge of the substrate is changed from electronegative to electropositive²⁶, which as a result enhances protein adsorption^{23,27}. Interestingly the regulatory role of electrostatic charge has been shown to supersede the hydrophilic effect, as substrates that have been electrostatically neutralised but still hold their super-hydrophilicity, do not retain their improvement in bioactivity²⁶. The decomposition or removal of organic contaminants in the form of hydrocarbons is another mechanism that has been proposed. Methylene hydrocarbons in the atmosphere are known to contaminate the surface of biomaterials²¹. Irradiation with UV light, either UVA or UVC, has been shown to reduce hydrocarbon content on TiO₂ materials^{24,28,41} and titanium,^{19-21,34} with UVC shown to be the more effective of the two light sources. In the present study the hydrocarbon content of CCMT substrates was tested using FTIR spectroscopy. The vibration bands of C-H bonds at 2853, 2923 and 2957cm⁻¹, which account to stretching modes of CH₂ and CH₃⁴¹, were not affected by 24 hours exposure to UVC light (Figure 3). This result does not coincide with a previous publication which was able to demonstrate a drop in the peak intensities of the same bonds on UV irradiated TiO₂ coated silicon²⁸. It may be that the UVC light used in this study was not powerful enough to decompose the hydrocarbons on the CCMT surface, although an additional UVC source was used to test this theory which also failed to reduce the peak intensities. Therefore it is unlikely that the UVC source is the cause of this anomaly, although this should not be ruled out entirely. Additionally, the FTIR equipment used in the present study may not have been sensitive enough to detect these small reductions in hydrocarbon content, or seeing as this is the first study to analyse CCMT created using APCVD, it may be that UVC light is not an effective way of reducing hydrocarbon content on substrates created using this technique. *Terriza et al* also observed improvement in cell adhesion and cytoskeletal structure in human osteoblasts on UV photofunctionalized amorphous TiO₂ with only a minor reduction in surface carbon content⁴². *Terriza et al* went on to dismiss the removal of hydrocarbons as the main cause for influencing this behaviour. Despite super-hydrophilicity being successfully achieved on UV photofunctionalized CCMT, the absence of significant hydrocarbon reduction may be connected to the less dynamic response observed from the human MSCs.

Conclusion

This study assessed the performance of human MSCs to ascertain if any improvement in cellular response could be achieved by functionalizing a TiO₂ coating on CCMT with UV light. The results indicated that UV photofunctionalization of CCMT enhanced specific markers related to adhesion. This included the promotion of larger cells with increased f-actin and vinculin expression (Figure 9), and superior cell retention on UV treated CCMT at both 3 and 24 hours (Figure 7). These results are highly advantageous for the field of orthopaedics, as MSCs that colonise at implant sites following surgery, should be better adhered to the surrounding surfaces, ultimately leading to a reduction in the amounts of dislodged cells that result from external forces such as blood flow and micro motion. Whilst other processes including proliferation, migration, attachment and differentiation were not affected by the UV photofunctionalization of CCMT, the enhancement in cellular adhesion markers alone should be sufficient to improve implant performance when compared against identical implants which have not undergone UV photofunctionalization.

Acknowledgments

This work was supported by EPSRC, Molecular Modelling and Materials Science Engineering Doctorate Centre UCL and Corin Ltd (Cirencester, UK).

References

1. S. Kurtz, K. Ong, E. Lau, F. Mowat and M. Halpern, *J. Bone Jt. Surg., Am. Vol.*, 2007, **89**, 780-785.
2. S. M. Kurtz, K. L. Ong, J. Schmier, F. Mowat, K. Saleh, E. Dybvik, J. Karrholm, G. Garellick, L. I. Havelin, O. Furnes, H. Malchau and E. Lau, *J. Bone Jt. Surg., Am. Vol.*, 2007, **89A**, 144-151.
3. K. L. Ong, F. S. Mowat, N. Chan, E. Lau, M. T. Halpern and S. M. Kurtz, *Clin. Orthop. Relat. Res.*, 2006, **446**, 22-28.
4. N. Logan, A. Sherif, A. J. Cross, S. N. Collins, A. Traynor, L. Bozec, I. P. Parkin and P. Brett, *J. Biomed. Mater. Res., Part A*, 2014, DOI: 10.1002/jbm.a.35264.
5. M. Geetha, A. K. Singh, R. Asokamani and A. K. Gogia, *Prog. Mater. Sci.*, 2009, **54**, 397-425.
6. R. Wang, K. Hashimoto, A. Fujishima, M. Chikuni, E. Kojima, A. Kitamura, M. Shimohigoshi and T. Watanabe, *Nature*, 1997, **388**, 431-432.
7. M. R. Khan, N. Donos, V. Salih and P. M. Brett, *Bone*, 2012, **50**, 1-8.
8. I. Wall, N. Donos, K. Carlqvist, F. Jones and P. Brett, *Bone*, 2009, **45**, 17-26.
9. G. Zhao, Z. Schwartz, M. Wieland, F. Rupp, J. Geis-Gerstorfer, D. L. Cochran and B. D. Boyan, *J. Biomed. Mater. Res., Part A*, 2005, **74A**, 49-58.
10. F. Schwarz, D. Ferrari, M. Herten, I. Mihatovic, M. Wieland, M. Sager and J. Becker, *J. Periodontol.*, 2007, **78**, 2171-2184.
11. F. Schwarz, M. Herten, M. Sager, M. Wieland, M. Dard and J. Becker, *Clin Oral Implants Res*, 2007, **18**, 481-488.
12. F. Schwarz, M. Herten, M. Sager, M. Wieland, M. Dard and J. Becker, *J. Clin. Periodontol.*, 2007, **34**, 78-86.
13. F. Schwarz, M. Wieland, Z. Schwartz, G. Zhao, F. Rupp, J. Geis-Gerstorfer, A. Schedle, N. Broggini, M. M. Bornstein, D. Buser, S. J. Ferguson, J. Becker, B. D. Boyan and D. L. Cochran, *J. Biomed. Mater. Res., Part B*, 2009, **88B**, 544-557.
14. D. Buser, N. Broggini, M. Wieland, R. K. Schenk, A. J. Denzer, D. L. Cochran, B. Hoffmann, A. Lussi and S. G. Steinemann, *J. Dent. Res.*, 2004, **83**, 529-533.
15. M. M. Bornstein, P. Valderrama, A. A. Jones, T. G. Wilson, R. Seibl and D. L. Cochran, *Clin Oral Implants Res*, 2008, **19**, 233-241.
16. N. P. Lang, G. E. Salvi, G. Huynh-Ba, S. Ivanovski, N. Donos and D. D. Bosshardt, *Clin Oral Implants Res*, 2011, **22**, 349-356.
17. N. Donos, S. Hamlet, N. P. Lang, G. E. Salvi, G. Huynh-Ba, D. D. Bosshardt and S. Ivanovski, *Clin Oral Implants Res*, 2011, **22**, 365-372.
18. H. Aita, W. Att, T. Ueno, M. Yamada, N. Hori, F. Iwasa, N. Tsukimura and T. Ogawa, *Acta Biomater.*, 2009, **5**, 3247-3257.
19. H. Aita, N. Hori, M. Takeuchi, T. Suzuki, M. Yamada, M. Anpo and T. Ogawa, *Biomaterials*, 2009, **30**, 1015-1025.
20. T. Ueno, M. Yamada, T. Suzuki, H. Minamikawa, N. Sato, N. Hori, K. Takeuchi, M. Hattori and T. Ogawa, *Biomaterials*, 2010, **31**, 1546-1557.
21. W. Atta, N. Hori, M. Takeuchi, J. Y. Ouyang, Y. Yang, M. Anpo and T. Ogawa, *Biomaterials*, 2009, **30**, 5352-5363.
22. W. Att, N. Hori, F. Iwasa, M. Yamada, T. Ueno and T. Ogawa, *Biomaterials*, 2009, **30**, 4268-4276.
23. N. Hori, T. Ueno, T. Suzuki, F. Iwasa, M. Yamada, W. Att, S. Okada, A. Ohno, H. Aita, K. Kimoto and T. Ogawa, *Int J Oral Maxillofac Implants*, 2010, **25**, 49-62.
24. T. Miyauchi, M. Yamada, A. Yamamoto, F. Iwasa, T. Suzawa, R. Kamijo, K. Baba and T. Ogawa, *Biomaterials*, 2010, **31**, 3827-3839.

25. T. Sawase, R. Jimbo, K. Baba, Y. Shibata, T. Ikeda and M. Atsuta, *Clin Oral Implants Res*, 2008, **19**, 491-496.
26. F. Iwasa, N. Hori, T. Ueno, H. Minamikawa, M. Yamada and T. Ogawa, *Biomaterials*, 2010, **31**, 2717-2727.
27. N. Hori, T. Ueno, H. Minamikawa, F. Iwasa, F. Yoshino, K. Kimoto, M. Lee and T. Ogawa, *Acta Biomater.*, 2010, **6**, 4175-4180.
28. M. Takeuchi, K. Sakamoto, G. Martra, S. Coluccia and M. Anpo, *J. Phys. Chem. B*, 2005, **109**, 15422-15428.
29. T. Zubkov, D. Stahl, T. Thompson, D. Panayotov, O. Diwald and J. Yates, *J. Phys. Chem. B*, 2005, **109**, 15454-15462.
30. A. J. Cross, C. W. Dunnill and I. P. Parkin, *Chem. Vap. Deposition*, 2012, **18**, 133-139.
31. G. Hyett, J. A. Darr, A. Mills and I. P. Parkin, *Chem. Eur. J.*, 2010, **16**, 10546-10552.
32. E. E. Golub and K. Boesze-Battaglia, *Curr. Opin. Orthop.*, 2007, **18**, 444-448.
33. R. Tsaryk, K. Peters, R. E. Unger, M. Feldmann, B. Hoffmann, F. Heidenau and C. J. Kirkpatrick, *J. R. Soc. Interface*, 2013, **10**, 20130428-20130428.
34. M. Yamada, T. Miyauchi, A. Yamamoto, F. Iwasa, M. Takeuchi, M. Anpo, K. Sakurai, K. Baba and T. Ogawa, *Acta Biomater.*, 2010, **6**, 4578-4588.
35. H. Minamikawa, T. Ikeda, W. Att, Y. Hagiwara, M. Hirota, M. Tabuchi, H. Aita, W. Park and T. Ogawa, *J. Biomed. Mater. Res., Part A*, 2013, DOI: 10.1002/jbm.a.35030.
36. K. Sunada, Y. Kikuchi, K. Hashimoto and A. Fujishima, *Environ. Sci. Technol.*, 1998, **32**, 726-728.
37. N. Hori, F. Iwasa, N. Tsukimura, Y. Sugita, T. Ueno, N. Kojima and T. Ogawa, *Acta Biomater.*, 2011, **7**, 3679-3691.
38. M. Textor, C. Sittig, V. Frauchiger, S. Tosatti, D. M. Brunette, in *Titanium in medicine*, ed. P. Tengvall, D.M. Brunette, M. Textor and P.Thomsen, Springer, New York, 2001, pp. 172-230.
39. J. D. Humphries, P. Wang, C. Streuli, B. Geiger, M. J. Humphries and C. Ballestrem, *J. Cell Biol.*, 2007, **179**, 1043-1057.
40. O. Carp, C. L. Huisman and A. Reller, *Progress in solid state chemistry*, 2004, **32**, 33-177.
41. P. A. Charpentier, K. Burgess, L. Wang, R. R. Chowdhury, A. F. Lotus and G. Moula, *Nanotechnology*, 2012, **23**, 425606.
42. A. Terriza, A. Díaz-Cuenca, F. Yubero, A. Barranco, A. R. González-Elipe, J. L. Gonzalez Caballero, J. Vilches and M. Salido, *J. Biomed. Mater. Res., Part A*, 2013, **101A**, 1026-1035.

Figure captions

Figure 1 Time course displaying the reduction in contact angle of ddH_2O on CCMT irradiated with UV light (*Above*). Error bars represent ± 1 standard deviation (SD) ($n = 5$).

Figure 2 Time course representing contact angle recovery of ddH_2O following the immediate removal of the CCMT substrates from UV exposure (*Above*). Error bars represent ± 1 SD ($n = 5$).

Figure 3 FTIR spectra of methylene hydrocarbon groups on CCMT before and after 24 hours UV exposure.

Figure 4 Proliferation of human MSCs in osteogenic media assessed by AlamarBlue over 21 days. A slight increase was observed in cell numbers on both substrates following the initial seeding, although cell numbers began to decline from day 12 onwards. Each line represents the mean ± 1 SD, $N = 3$, $n = 3$.

Figure 5 Proliferation of human MSCs in GM assessed by AlamarBlue until 21 days. UV treatment of CCMT prior to seeding the MSCs did not have an effect on the proliferative ability of the cells. Each line represents the mean ± 1 SD, $N = 3$, $n = 3$.

Figure 6 Evaluation of cell attachment after 24 hours in culture. No difference between UV treated and non-UV CCMT substrates was observed. Each column represents the mean ± 1 SD, $N = 3$, $n = 3$.

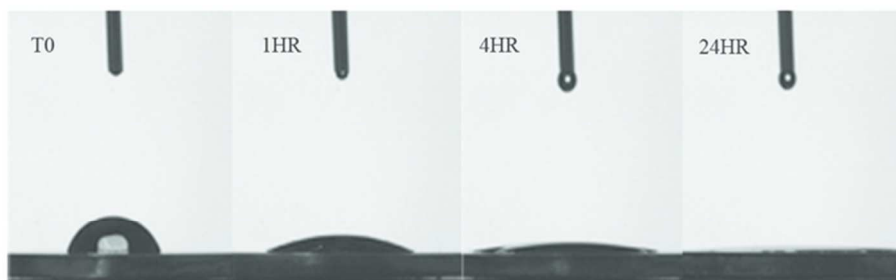
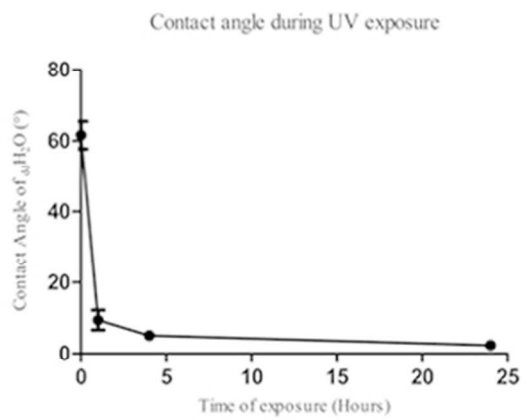
Figure 7 Evaluation of cell retention, displaying the remaining cell population following three washes in PBS after 3 and 24 hours incubation. The UV treated substrate was shown to have a greater remaining cell population. Each column represents the mean \pm 1 SD, N = 3, n = 3. * = p < 0.05.

Figure 8 Evaluation of cell migration, displaying the migratory cell populations after a 4.5 hour incubation period. There was no difference between UV treated and non-UV CCMT substrates. Each column represents the mean \pm 1 SD, N = 3, n = 3.

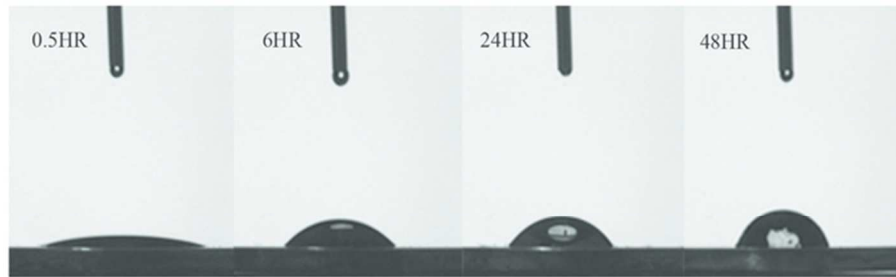
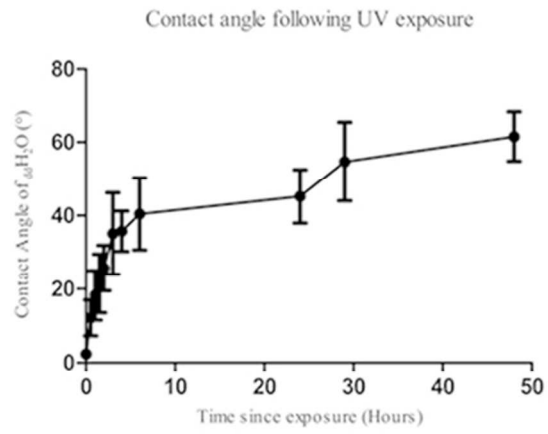
Figure 9 Fluorescent microscopy images displaying the cytoskeletal organisation of MSCs on non-UV (A, C, E) and UV-treated (B, D, F) CCMT substrates after incubation for 24 hours in OM. MSCs are noticeably larger on UV treated CCMT, with more developed actin fibres. Green depicts f-actin (A B), whilst red shows vinculin expression (C D). Images were taken at X 40. Scale bar = 50 μ m. Online Version in colour.

Figure 10 Cytomorphometric analysis of actin (A), vinculin (B), cell perimeter (C) and ferets diameter (D) of human MSCs after 24 hours culture in OM. Each column represents the mean \pm 1SD, n = 13. * = p < 0.05.

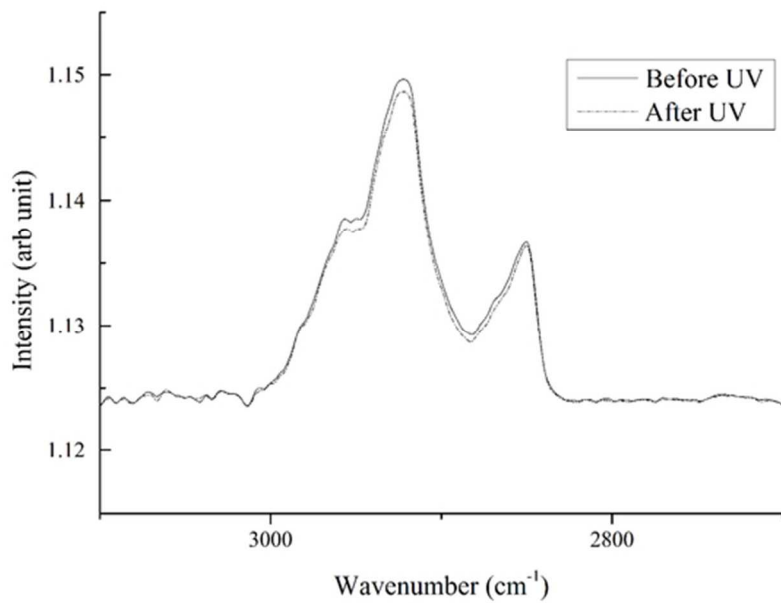
Figure 11 Markers of mineralisation were studied, showing ALP activity (A), calcium ion content (B) and hydroxyapatite formation (C). No significant difference was observed between UV treated and non-UV substrates for all markers. Fluorescent microscopy analysis of hydroxyapatite was also performed and showed no apparent difference in deposition between non UV CCMT (D) and UV treated CCMT (E). Each column represents the mean \pm 1SD, N = 3, n = 3. Scale bar = 200 μ m. Online version in colour.



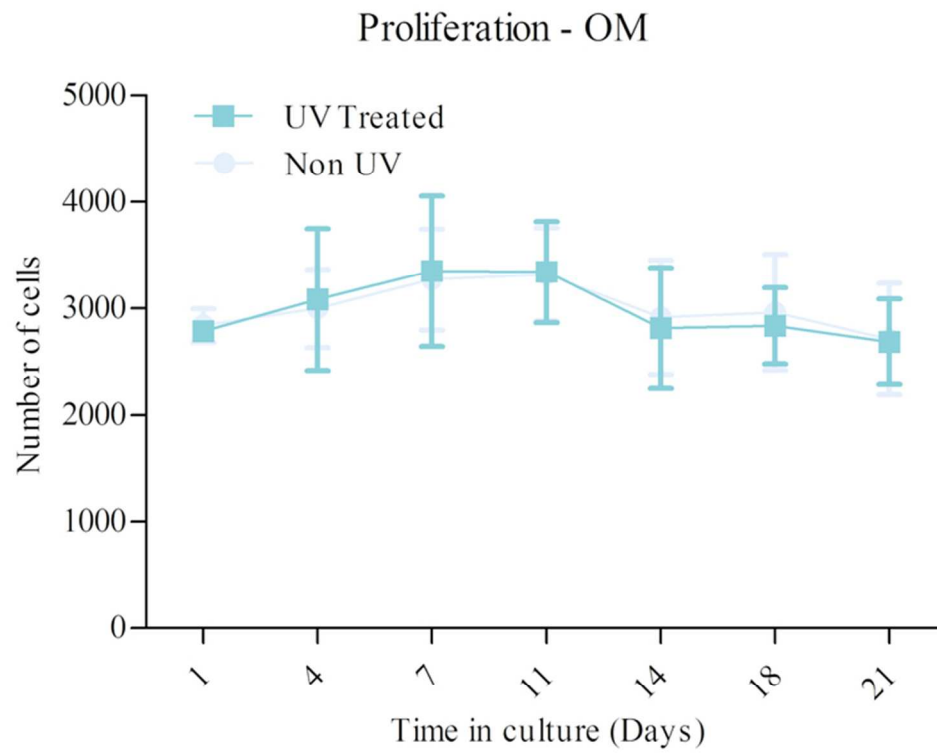
63x49mm (300 x 300 DPI)



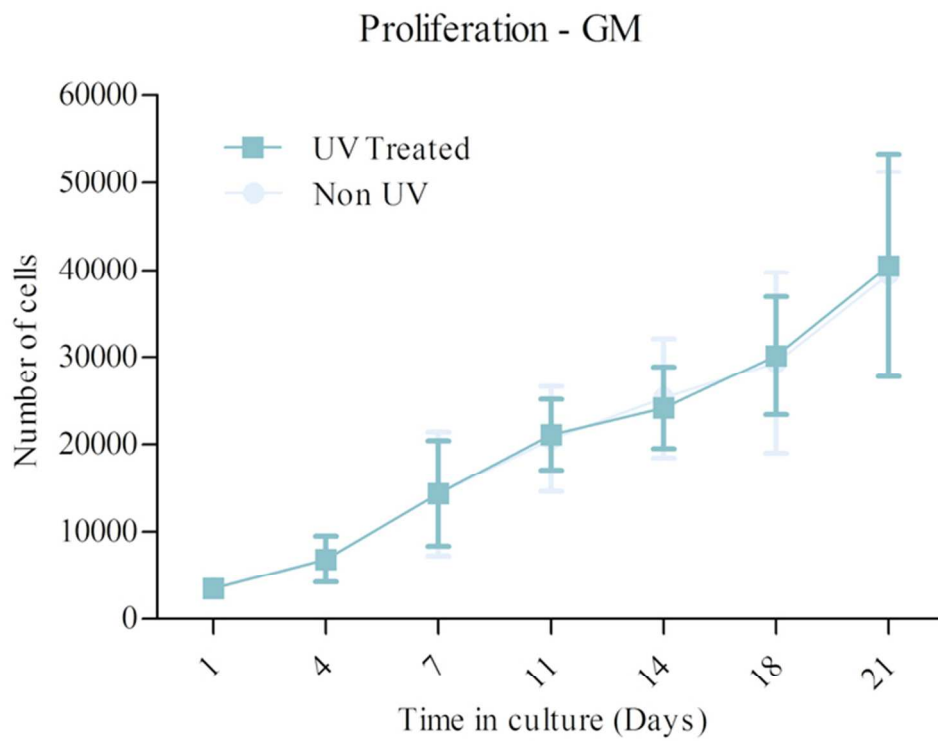
63x49mm (300 x 300 DPI)



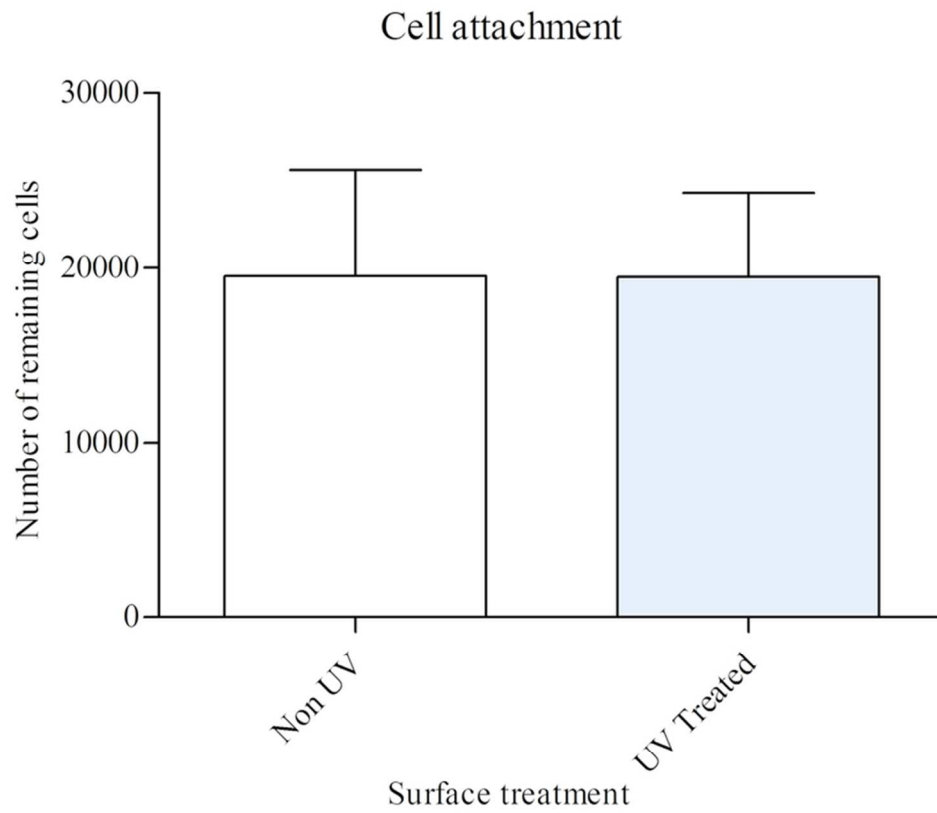
57x40mm (300 x 300 DPI)



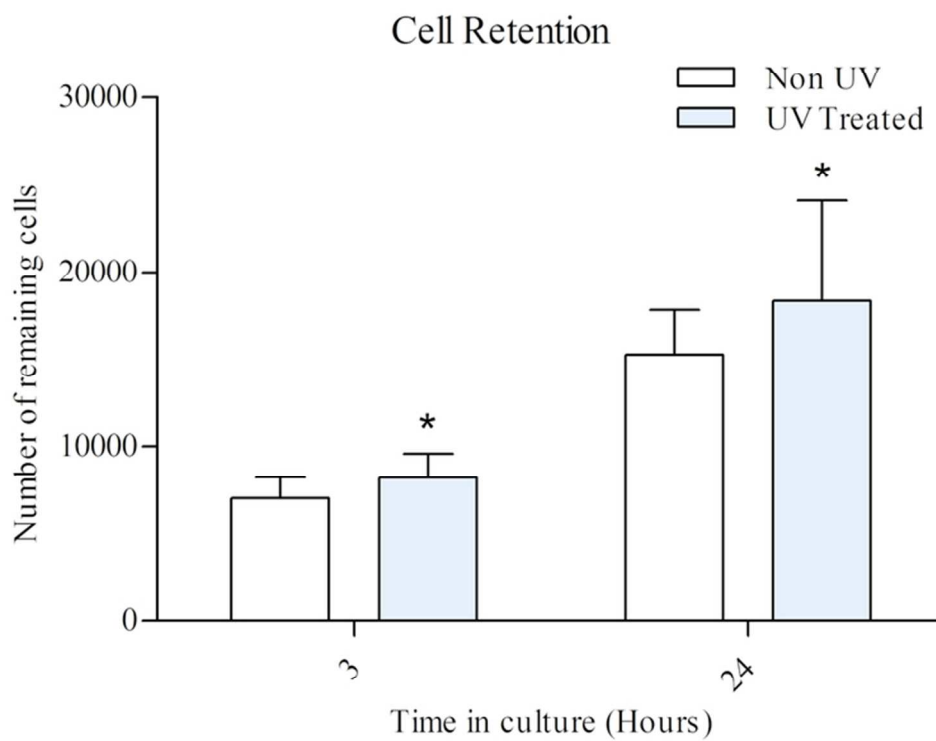
67x55mm (300 x 300 DPI)



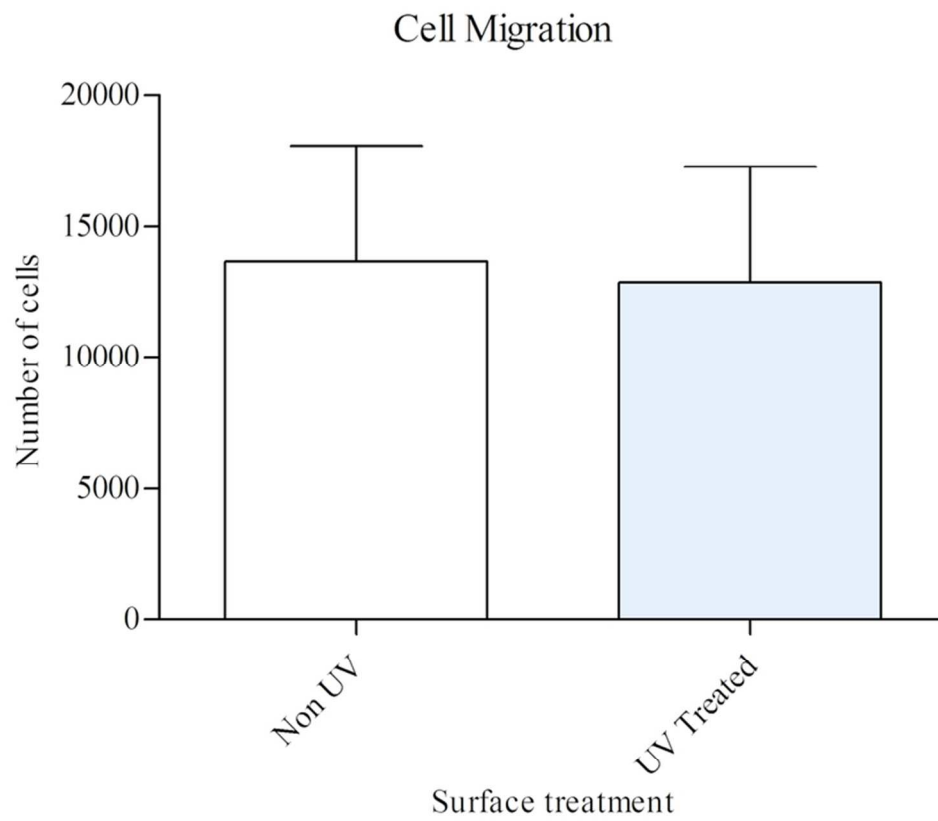
66x53mm (300 x 300 DPI)



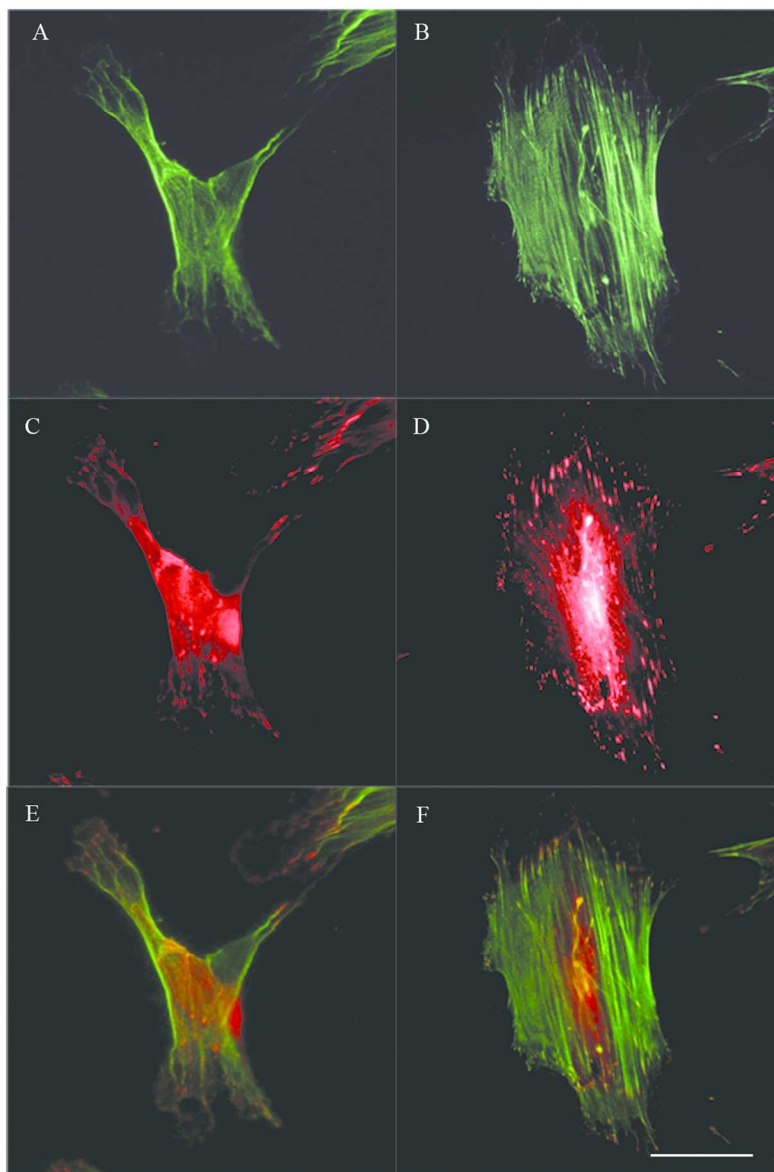
73x64mm (300 x 300 DPI)



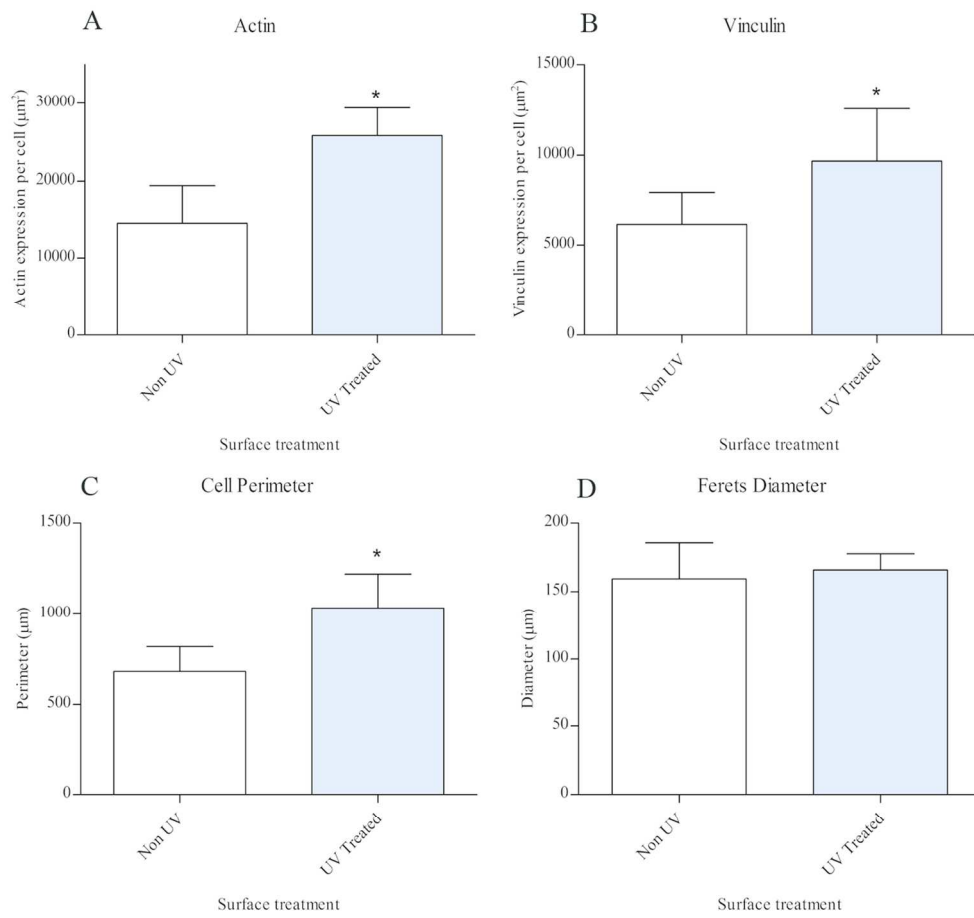
66x53mm (300 x 300 DPI)



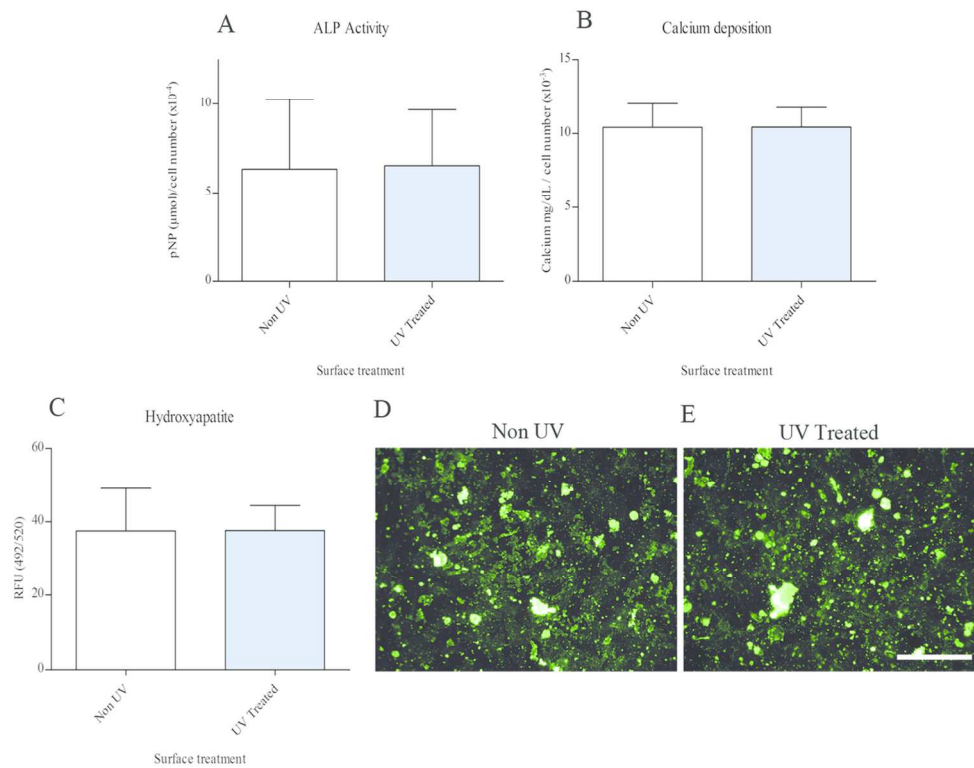
73x65mm (300 x 300 DPI)



122x181mm (300 x 300 DPI)



147x136mm (300 x 300 DPI)



122x93mm (300 x 300 DPI)

Graphical Abstract

Markers of cell adhesion in human mesenchymal stem cells were shown to be enhanced on TiO₂ coated CoCrMo substrates that had undergone UV-photofunctionalization for 24 hours. Cells were larger, with superior f-actin and vinculin formation and promoted greater cell retention at both 3 and 24 hours. UV-photofunctionalization of TiO₂ coated implant surfaces may prove advantageous by supporting the colonisation and adhesion of cells capable of facilitating in bone healing.

